Unsteady High-Speed MHD Natural Convective Flow over an Inclined Plate with Variable Electrical Conductivity, Higher-order Chemical Reaction, Thermal Radiation, and Concentration Gradient-Dependent Heat Generation/Absorption

IGHOROJE W. A. OKUYADE
Department of Mathematics/Statistics,
Federal Polytechnic of Oil and Gas,
Bonny,
NIGERIA

ORCiD: https://orcid.org/0003-0011-0019-1160

Abstract: - The problem of unsteady high-speed MHD natural convective flow over an inclined plate in a fluid with variable electrical conductivity, higher-order chemical reaction, thermal radiation, and concentration gradient-dependent heat generation/absorption is investigated. It is assumed that the fluid is chemically reactive, and of the nth-order; electrically and magnetically conducting; viscous, incompressible, and Newtonian; the plate is highly porous, thermally and electrically conductive, and heated to a high-temperature regime to emit thermal rays; the plate is heated at the bottom, and the heat is conducted to the top such that convection currents exist. The equations governing the flow are non-linear and coupled partial differential equations. They are transformed into ordinary differential equations using the time-dependent similarity transformation, and solved by the Modified Homotopy Perturbation approach. Expressions for the concentration, temperature, velocity, rates of heat and mass transfer, and the stress/force on the wall are obtained, computed, and presented graphically and quantitatively for the different parameters. The analysis of results shows among others, that the increase in the: order of chemical reaction parameter causes fluctuation in the fluid concentration structure, but increases the flow velocity; the Forchheimer number decreases the fluid velocity, but increases the force on the surface wall; electrical conductivity causes fluctuation in the temperature structure, increases the rate of heat transfer to the fluid, and decreases the force on the wall; inclined angle decreases the fluid velocity.

Key-Words: - Electrical conductivity, Higher-order **c**hemical reaction, High speed, MHD, Natural convection, Suction, Heat generation/absorption, Thermal radiation.

Received: June 19, 2024. Revised: September 25, 2024. Accepted: November 28, 2024. Published: December 31, 2024.

1 Introduction

Natural convective heat transfer in the presence of MHD high speed has significant applications in science and engineering. It is relevant in astrophysics, biomedical engineering (cardiac magnetic resonance imaging (MRI), electrocardiogram (ECG)), crystal growth, enhanced crude oil recovery and refining, gas-cooled reactor safety, geophysics, and geothermal reservoirs, material processing and cooling reactors, nuclear power reactors, solar structures, welding, and the likes.

Depending on the situation, different parameters affect flows. In the quest to understand flow situations researches are carried out to examine the roles of concerned parameters, hence there exist many reports in this domain of study. A chemical reaction is initiated by the difference in the concentration of mixing species/substances. An interesting aspect of the chemical reaction is the order of the chemical reaction. The order of a chemical reaction is proportional to the powers to which the concentration is raised. The phenomenon of higher-order chemical reactions has applications in plastic curing; food processing; pulp, polymer, insulated cable manufacturing, etc. A good number of research works exist on the flow involving higher-order chemical reactions over vertical and inclined moving plates. For example, [1] considered the MHD mixed convective nth-order chemically reacting flow; [2] looked at the flow involving the nth-order chemical reaction in the presence of viscous dissipation; [3] considered the MHD

Nanofluid flow with higher order chemical reaction and slip boundary conditions.

Among the forces (internal and external) affecting fluid flow is electricity. A chemically reacting fluid is a base/alkaline, acid, or a mixture of both. It is electrolytic, therefore, its particles are positively, or negatively charged. The motion of the particles in the presence of a magnetic field generates electric currents. The conduction of electricity in a fluid depends on the number of ions per unit volume and their drift density. The drift density of an ion varies with the electric field intensity and the mass of the ion. Therefore, the electrical conductivity of a fluid is a measure of how much voltage is required for an electric current to flow. For application, electrical conductivity has great relevance in metallurgical process control. Some literature exists on the flow over vertical plates with variable electrical conductivity and MHD. For instance, [4] studied numerically the flow situation when the plate is isothermal, and observed that an increase in the heat generation parameter increases the fluid temperature, velocity, and wall shear stress; an increase in the electrical conductivity parameter increases the fluid velocity, wall shear stress and the rate of heat transfer but decreases the fluid temperature; an increase in the Hartmann number increases the fluid temperature but decreases the flow velocity and the rate of heat transfer; an increase in the Prandtl number increases the wall shear stress; [5] numerically examined the flow over an inclined stretching sheet with variable chemical reaction, variable electrical conductivity, variable heat and mass fluxes, and cross-diffusion effects. [6] examined the steady 2-D flow over an isothermal porous plate with variable electrical conductivity using a numerical approach and observed among others that an increase in electrical conductivity decreases the fluid velocity.

The speed at which a fluid flows is dependent on the level of interaction of its particles, which is influenced by many parameters/factors. In fluid dynamics, the high-speed situation exists in many facets, such as in gas dynamics, hydrodynamics, and porous media flow. Specifically, porous media may be classified into homogeneous and non-homogeneous. It is homogeneous when the ratio of the pore area to the total area of the solid boundary is constant, and non-homogeneous/heterogeneous when the ratio of the pore area to the total area of the boundary is not constant. For its relevance, the high-speed flow past vertical and inclined porous surfaces has been investigated by many research workers. For example, [7] and [8]) investigated the natural convective boundary layer high-speed flow using the finite difference method, and observed that magnetic field increases temperature; [9] examined the natural convective high-speed flow over a vertical stretching sheet under the influence of thermal diffusion using finite difference numerical method and found that high-speed MHD enhances the temperature. In combination with electrical conductivity, thermal radiation, and high-order chemical reaction, [10] investigated the transient MHD high-speed flow over an inclined exponentially moving porous plate with radiation absorption and variable electrical conductivity effects using the method of explicit finite difference numerical approach, and observed that the magnetic field enhances the temperature but freezes the velocity, skin friction, and Nusselt number; Dufour number increases the concentration profiles. Furthermore, neglecting the effects of electrical conductivities and the Forchheimer parameter, [11] considered MHD natural convective flow over an oscillatory vertical porous plate with thermal radiation, heat, and mass absorption effects using the explicit finite difference method.

The position of a moving object in a flow system may affect its motion and that of the fluid. Some literature exists on the flow past an inclined plate, For example, [11], by the exact analysis of radiation, studied the convective flow with heat and mass transfer over an inclined plate in a porous medium; [12] examined the mass transfer and heat generation effects on MHD free convective flow past an inclined vertical surface in a porous medium; [13] investigated the heat and mass transfer effects on a steady MHD free convective dissipative fluid flow past an inclined porous surface with heat generation using the Lie analysis approach; [14] considered the influence of variable permeability on the unsteady MHD convection flow past a semi-infinite inclined plate with thermal radiation and chemical reaction; [15] looked into the MHD free convective flow and mass transfer flow with heat generation through an inclined plate. [16] studied the mass transfer flow through an inclined plate with porous medium; [17] analyzed the unsteady natural convective flow through an inclined plate; [18] examined the radiation and mass transfer effects on MHD flow through porous medium past an exponentially accelerated inclined plate with variable temperature; [19] considered the radiation absorption and variable electrical conductivity effects on high-speed MHD free convective flow past an exponentially accelerated inclined plate.

As a wide and inexhaustive domain of study, the fluid flow over vertical porous plates also has been

torch-lighted in different perspectives by other researchers among whom are [20], [21], [22], [23], [24], [25], [26], [27], [28], [29], [30], [31], [32], [33], [34], [35], [36], [37], [38].

Notably, [6] studied numerically the steady 2-D flow over an isothermal porous plate with variable electrical conductivity. Their work has some deficiencies. Therefore, this work extends it by considering the unsteadiness, and a high-speed case in the presence of higher-order chemical reaction, thermal radiation, inclined angle, and concentration gradient-dependent heat generation/absorption using an analytic approach.

2 Problem Formulation

2.1 Mathematical Foundation

The Darcy-Forchheimer Model for Flow through Cracks/Faults in Rock Matrixes

Through Henry Darcy's experimental results on the flow of water through sand beds/aquifers the Darcy law, which links pressure drop with velocity, the fluid flow through porous media was initiated. This law became applicable to the flow of gas, water, and oil through petroleum reservoirs, and it is prescribed as:

$$-\nabla p = \frac{\mu}{\kappa} u = \chi^2 u \tag{1}$$

where χ^2 is the porosity of the medium.

However, studies have shown that the Darcy linear model cannot hold in the presence of higher velocities. Upon this, an inertial term representing the kinetic energy called the Forchheimer term was modeled into the Darcy law/equation to form the Darcy-Forchheimer mode, [38], as:

$$-\nabla p = \frac{\mu}{\kappa} u + \gamma \rho u^2 \tag{2}$$

where γ is the non-Darcy coefficient prescribed as $\gamma = \omega \kappa^r$, and is a function of dynamic viscosity and permeability, [39], ω a constant, κ the permeability of the porous media, and r an index, [40]. For engineering purposes, $\gamma = \frac{m}{\sqrt{\kappa}}$, m is the Forchheimer coefficient, or drag coefficient of the fluid, [41]. Also, for γ zero, the model reduces to the Darcy's law. The Darcy-Forchheimer model is used for studying flow through pores and cracks in the aquifers/reservoirs, [42]. Furthermore, by extension, the introduction of the Forchheimer term into the Navier-Stokes equation gives the Navier-Stokes model for high-speed flow through porous media, as shall be seen later.

The basic assumptions of the Darcy-Forchheimer model are: that the flow is macroscopic and one-dimensional; the porous medium is homogeneous and isotropic, and the fluid is incompressible.

2.2 Physics of Problem and Mathematical Formulation

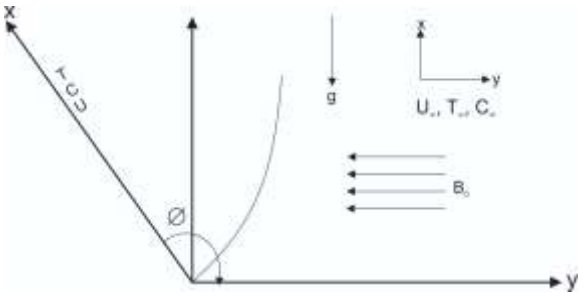

Fig. 1: The schematic of a vertically accelerating plate in a fluid

Unsteady high-speed MHD natural convective flow over an inclined plate with variable electrical conductivity, higher-order chemical reaction, thermal radiation, and concentration gradient-dependent heat generation/absorption is considered. The schematic of the flow is shown in Figure 1.The model is formulated on the assumption that the fluid is Newtonian, viscous and incompressible, chemically reactive and of higher-order, electrically conducting, and thermally radiating and optically thin; the plate is porous, vertically inclined, heated to a high-temperature regime such that radiant rays are emitted; the heat flux is acting in a direction perpendicular to the plate; there is a convective temperature gradient between the bottom and upper surface of the plate with a heat source at the bottom and sink at the top, such that the flow is naturally convective; a magnetic field of constant magnitude but with negligible induction (when compared to the applied magnetic field) is applied perpendicularly to the flow direction; the negligible magnetic field rendered the magnetic Reynolds number insignificant; the suction at the wall is of a constant magnitude; the flow is of a high speed, as such the Forchheimer factor is invoked. In this model, the x-axis is in the vertical direction of the plate and the y-axis is normal to it; u is the velocity along the x-axis, and is parallel to or along the plate, and v is the velocity along the y-axis, and it is assumed a suction

at the wall. Therefore, if (u', v') are the velocity components in the spatial direction (x', y', t'); T_∞ and C_∞ are the ambient at $t' \le 0$; T_w and C_w temperature and concentration at the wall of the plates, and T' and C' are the fluid temperature at $t' > 0$. Then, by the Boussinesq's approximations, the unsteady 2-D governing equations of mass balance, momentum, energy and mass diffusion are:

$$\frac{\partial u'}{\partial x'} + \frac{\partial v'}{\partial y'} = 0 \tag{3}$$

$$\rho\left(\frac{\partial u'}{\partial t'} + u\frac{\partial u'}{\partial x'} + v\frac{\partial u'}{\partial y'}\right) = \mu\frac{\partial^2 u'}{\partial y'^2} + \rho g\beta_t\left(T' - T_\infty\right)\cos\phi$$

$$+ \rho g\beta_C\left(C' - C_\infty\right)\cos\phi \; - \sigma_e' B_o{}^2 u' - \frac{\mu}{\kappa}u' - \frac{\lambda}{\kappa}u'^2 \tag{4}$$

$$\rho C_p\left(\frac{\partial T'}{\partial t'} + u\frac{\partial T'}{\partial x'} + v\frac{\partial T'}{\partial y'}\right) = k\frac{\partial^2 T'}{\partial y'^2} - \frac{\partial q_r'}{\partial y'}$$

$$+ Q'\frac{\partial C'}{\partial y'} + \sigma_e' B_o^2 u^2 \tag{5}$$

$$\frac{\partial C'}{\partial t'} + u'\frac{\partial C'}{\partial x'} + v'\frac{\partial C'}{\partial y'} = D\frac{\partial^2 C'}{\partial y'^2} - k_r\left(C' - C_\infty\right)^n \tag{6}$$

with the boundary conditions

$$t < 0: \quad u' = 0, v' = 0, T' = T_\infty, C' = C_\infty \text{ for all y} \tag{7}$$

$$t > 0: u' = 0, v' = 0, T' = T_w, C' = C_w \text{ at } y' = 0 \tag{8}$$

$$u' = 0, T' \to T_\infty, C' \to C_\infty \text{ at } \quad y' \to \infty \tag{9}$$

where ρ is the fluid density, μ is the dynamic viscosity, $\lambda(=\gamma\rho)$ is the empirical constant, as given above; g is the acceleration due to gravity; σ_e' electrical conductivity of the fluid; $B_o{}^2$ is the magnetic field flux; β_t is the thermal volumetric expansion of the fluid; β_C is the species volumetric expansion of the fluid; ϕ is the inclination angle; k thermal conductivity; k_r is the chemical reaction rate constant; q_r' is the thermal radiation flux; D_m is the molecular diffusivity coefficient of the fluid; C_p is the specific heat capacity of the fluid at constant pressure; Q' is the heat generation/absorption constant, or the heat source/sink strength of the plate, and is negative for heat absorption and positive for heat generation; n is the order of a chemical reaction.

Electrical conductivity is prescribed in different0 forms, and as a function of temperature, can be given for liquids as:

$$\frac{1}{\sigma_e} = \frac{1}{\sigma_e'}\left[1 + \xi'\left(T' - T_\infty\right)\right] \tag{10}$$

where ξ' is the constant based on the electrical conductivity property of the fluid.

Substituting equation (10) into equation (4), gives:

$$\rho\left(\frac{\partial u'}{\partial t'} + u\frac{\partial u'}{\partial x'} + v\frac{\partial u'}{\partial y'}\right) = \mu\frac{\partial^2 u'}{\partial y'^2} + \rho g\beta_t\left(T' - T_\infty\right)\cos\phi$$

$$+ \rho g\beta_C\left(C' - C_\infty\right)\cos\phi - \sigma_e' B_o{}^2 u' - \frac{\mu}{\kappa}u' - \frac{\lambda}{\kappa}u'^2 \tag{11}$$

Thermal radiation, as a process of heat propagation using electromagnetic waves, occurs due to high-temperature differences. It is a heat transfer comparable to convective heat transfer. Thermal radiation analysis is based on the limits of optical depth (the distance a photon travels in a fluid before something happens to it) or penetration of the thermal radiant rays into a fluid. It is optically thin when the photon travels a long distance in the fluid, and is the case where the fluid is transparent with relatively low density, or optically thick when a photon travels a short distance in the fluid, and is the case where the fluid is not transparent and the density is large. In terms of absorption, if the thermal radiation energy is emitted into the fluid but is not absorbed, the fluid media is said to be non-participating or optically thin. On the other hand, if the thermal rays emitted into the fluid are absorbed at the fluid boundaries, the fluid is said to be participating or optically thick. Radiation heat fluxes can be approximated using the Roseland diffusion approximations. For an optically thin fluid, the radiation heat flux can be prescribed as:

$$q_r' = -\frac{4\sigma}{3\alpha}\frac{\partial T'^4}{\partial y'}$$

where σ is the Stefan-Botzmann constant, α is the mean absorption coefficient.

Assuming the temperature changes within the adjacent fluid layers are small enough that T'^4 can be expanded as a linear function of the temperature. Then expanding T'^4 in the Taylor series about T_∞, and ignoring the higher order terms, we have:

$$q_r' = -\frac{4\sigma}{3\alpha}\frac{\partial T'^4}{\partial y'}$$

$$q_r' = \frac{-16\sigma T_\infty^3}{3\alpha}\frac{\partial T'}{\partial y'} \quad (12)$$

such that:

$$\frac{\partial q_r'}{\partial y} = \frac{-16\sigma T_\infty^3}{3\alpha}\frac{\partial^2 T'}{\partial y'^2} \quad (13)$$

Substituting equations (10) and (13) into equation (5) gives:

$$\frac{\partial T'}{\partial t'} + u'\frac{\partial T'}{\partial x'} + v'\frac{\partial T'}{\partial y'} = \frac{k}{\rho C_p}\frac{\partial^2 T'}{\partial y'^2} + \frac{16\sigma T_\infty}{\rho C_p 3\alpha}\frac{\partial^2 T'}{\partial y'^2} + \frac{Q'}{\rho C_p}\frac{\partial C'}{\partial y'} + \frac{\sigma_e {B_o}^2}{\rho C_p\left[1+\xi'\left(T'-T_\infty\right)\right]}u'^2 \quad (14)$$

We introduce the following non-dimensionalized quantities:

$$y = \frac{y'U_o}{\upsilon}, u = \frac{u'}{U_o}, t = \frac{t'{U_o}^2}{\upsilon}, \Theta = \frac{T'-T_\infty}{T_w - T_\infty},$$

$$\Phi = \frac{C'-C_\infty}{C_\infty - C_\infty}, Gr = \frac{gB_t(T_w - T_\infty)\upsilon}{{U_o}^3},$$

$$Gc = \frac{gB_C(C_w - C_\infty)\upsilon}{{U_o}^3}, M = \frac{\sigma_e B_o^2}{\rho {U_o}^2},$$

$$Da = \frac{kU_o}{\upsilon^2}, F_S = \frac{\lambda U_o}{\rho\upsilon}, \Pr = \frac{\mu C_p}{k},$$

$$Q_1 = \frac{Q'}{\rho C_p U_o}, Ra = \frac{4\sigma T_\infty^3}{\alpha k},$$

$$Sc = \frac{\upsilon}{D}, \delta = \frac{k_r}{U_o}, \xi = \xi'(T_w - T_\infty) \quad (15)$$

where Θ is the dimensionless temperature, Φ is the dimensionless concentration, Da is the Darcy number, Ec is the Eckert number, F_S is the Forchheimer parameter, Gr is the Grashof number due to temperature, Gc is the Grashof number due to concentration, M is the Hartmann number, $\Pr$ is the Prandtl number, Ra is the Raleigh number, Q_1 is the heat absorption parameter, Sc is the Schmidt number, U_o is the velocity of the external flow at infinity, χ^2 is the porosity parameter, δ is the chemical reaction rate parameter, υ is the kinematic viscosity.

Substituting equation (15) into equations (3), (6), (11), (14), (8) and (9) gives:

$$\frac{\partial u}{\partial x} + \frac{\partial v}{\partial y} = 0 \quad (16)$$

$$\frac{\partial u}{\partial t} + u\frac{\partial u}{\partial x} + v\frac{\partial u}{\partial y} = \frac{\partial^2 u}{\partial y^2} - \left(\frac{M}{1+\xi\Theta} + \frac{1}{Da}\right)u - \frac{F_S}{Da}u^2 + Gr\Theta Cos\varphi + Gc\Phi Cos\varphi \quad (17)$$

$$\frac{\partial \Theta}{\partial t} + u\frac{\partial \Theta}{\partial x} + v\frac{\partial \Theta}{\partial y} = \frac{1}{\Pr}\left(1+\frac{4}{3}Ra\right)\frac{\partial^2 \Theta}{\partial y^2} + Ec\left(\frac{M}{1+\xi\Theta}\right)u^2 + Q_1\frac{\partial \Phi}{\partial y} \quad (18)$$

$$\frac{\partial \Phi}{\partial t} + u\frac{\partial \Phi}{\partial x} + v\frac{\partial \Phi}{\partial y} = \frac{1}{Sc}\frac{\partial^2 \Phi}{\partial y^2} - \delta^2 \Phi^n \quad (19)$$

with the boundary conditions

$$t > 0: u = 0, v = 0, \Theta = 1, \Phi = 1 \text{ at } y = 0 \quad (20)$$

$$u = 0, v = 0, \Theta = 0, \Phi = 0 \text{ at } y \to \infty \quad (21)$$

Fluid dynamical problems are usually highly coupled and not easily solved sets of partial differential equations. To make the problems tractable, similarity transformations are used to first reduce them to ordinary differential equations. Similarity transformations are of different forms and are subject to modifications, provided the prescribed equations of mass balance are satisfied. Now, simplifying equations (17) - (19) into ordinary differential equations, we used the modified time-dependent similarity transformation of the form:

$$u = \frac{\partial \psi}{\partial y} = \frac{A}{t}xf'(\eta), v = -\frac{\partial \psi}{\partial x} = -A\sqrt{\frac{\upsilon}{t}}f(\eta), \quad \eta = y\sqrt{\frac{1}{\upsilon t}} \quad (22)$$

[43],

and the suction

$$v = -A\sqrt{\frac{\upsilon}{t}}f(0), s = f(0) \quad (23)$$

is the suction/injection, [43];
where $v = s = 0$ is for impermeable surface, $v = s < 0$ is for suction (the fluid flows towards the

plate), and $v = s > 0$ is for injection (the fluid moves from the plate.

Substituting equations (22) and (23) into equations (16) - (21), we have:

$$f''' + \left(\frac{1}{2}\eta + s\right) f'' - \left(1 + \frac{F_S}{Da}\right) f'^2 - \left(\frac{M}{1+\xi\Theta} + \frac{1}{Da}\right) f' = -Gr\Theta\cos\phi - Gc\Phi\cos\phi \quad (24)$$

$$\frac{1}{\Pr}\left(1 + \frac{4}{3}Ra\right)\Theta'' + \left(\frac{1}{2}\eta + s\right)\Theta' - f'\Theta = -Ec\left(\frac{M}{1+\xi\Theta}\right) f'^2 + Q_1\Phi' \quad (25)$$

$$\frac{1}{Sc}\Phi'' + \left(\frac{1}{2}\eta + s\right)\Phi' + f'\Phi = \delta\Phi^n \quad (26)$$

Equation (16) is satisfied by the stream function.

By the prescribed suction, the boundary conditions can be derived as:

$$f = s,\ f' = 1, \Theta = 1, \Phi = 1 \text{ at } \eta = 0 \quad (27)$$

$$f = 0, \Theta = 0, \Phi = 0 \text{ at } \eta \to \infty \quad (28)$$

Similarly, other factors affecting the flow are the Nusselt number (Nu), Sherwood number (Sh), and Skin friction (Cf) prescribed non-dimensionally as:

$$Nu = -\Theta'\big|_{\eta=0} \quad (29)$$

$$Sh = -\Phi'\big|_{\eta=0} \quad (30)$$

$$Cf = \mu f''\big|_{\eta=0} \quad (31)$$

3 Problem Solution

3.1 Method of Solution

An examination of equations (24) - (26), depicts that they are non-linear and coupled. To make them tractable, we opt to use the Modified Homotopy Perturbation Method in the form:

$L(v) + N(v) = f(r), r\Xi\Omega$

with the boundary condition:

$$B\left(u, \frac{\partial u}{\partial y}\right) = 0, r\Xi\Gamma$$

where L is a linear operator, N is a nonlinear operator, B is a boundary operator, Γ is the boundary of the domain Ω, $f(r)$ is a known analytic function. For a Homotopy Perturbation technique, He (a Chinese) constructed a homotopy:

$v(r, p) = \Omega[0,1] \to R$

which satisfies:

$$H(v, p) = (1-p)[L(v) - L(u_O)] + p[L(v) + N(v) - f(r)] = 0$$

where $p\Xi[0,1]$ is an impending parameter, u_O is an initial approximation that satisfies the boundary conditions. Clearly, from the above equation, we have:

$H(v,0) = [L(v) - L(u_O)] = 0$,

$H(v,1) = [L(v) + N(v) - f(r)] = 0$

Importantly, the process of changing p from zero to unity $v(r, p)$ is like that of changing from $u_O(r)$ to $u(r)$, and this is called a *deformation* in *Topology*; the $[L(v) - L(u_O)] = 0$ and $[L(v) + N(v) - f(r)] = 0$ are called homotopic.

Here, the basic assumption is that the solution of the equation can be expressed as a power series in p:

$v = v_O + pv_1 + p^2 v_2 + \ldots$ ([37], [44]).

The difference between HPM and MHPM is seen in their use of boundary conditions. In HPM, order zero takes the boundary conditions at t<0, order one takes the boundary conditions at t>0 for y=0, and order two takes that at t>0 for y=∞, while in MHPM all the orders use the boundary conditions at t>0: y=0 and y=∞ but with little modifications, as we shall see below.

Based on the given analysis, writing equations (24) - (26) in MHPM form, we have:

$$(1-p) f''' + p \begin{bmatrix} f''' + \left(\frac{1}{2}\eta + s\right) f'' - \left(1 + \frac{F_S}{Da}\right) f'^2 \\ - \left(\frac{M}{1+\xi\Theta} + \frac{1}{Da}\right) f' + Gr\Theta\cos\phi \\ + Gc\Phi\cos\phi \end{bmatrix} = 0 \quad (32)$$

$$\frac{1}{\Pr}\left(1+\frac{4}{3}Ra\right)\Theta''+p\left[\begin{array}{l}\left(\frac{1}{2}\eta+s\right)\Theta'-f'\Theta\\+Ec\left(\frac{M}{1+\xi\Theta}\right)f'^{2}-Q_1\Phi'\end{array}\right]=0 \quad (33)$$

$$(1-p)\frac{1}{Sc}\Phi''+p\left[\begin{array}{l}\frac{1}{Sc}\Phi''+\left(\frac{1}{2}\eta+s\right)\Phi'-f'\Phi\\-\delta\Phi^{n}\end{array}\right]=0 \quad (34)$$

Expanding these gives:

$$(1-p)\frac{1}{Sc}\Phi''+p\left[\begin{array}{l}\frac{1}{Sc}\Phi''+\left(\frac{1}{2}\eta+s\right)\Phi'-f'\Phi\\-\delta\Phi^{n}\end{array}\right]=0 \quad (35)$$

$$f'''=-p\left[\begin{array}{l}\left(\frac{1}{2}\eta+s\right)f''-\left(1+\frac{F_s}{Da}\right)f'^{2}\\-\left(\frac{M}{1+\varepsilon\Theta}+\frac{1}{Da}\right)f'+Gr\Theta\cos\phi\\+Gc\Phi\cos\phi\end{array}\right] \quad (36)$$

$$\frac{1}{Sc}\Phi''=-p\left[\left(\frac{1}{2}\eta+s\right)\Phi'-f'\Phi-\delta\Phi^{n}\right] \quad (37)$$

Furthermore, the dependent variables are expressed in series expansion as:

$$f=f_o+pf_1+p^2f_2+.. \quad (38)$$

$$\Theta=\Theta_o+p\Theta_1+p^2\Theta_2+.. \quad (39)$$

$$\Phi=\Phi_o+p\Phi_1+p^2\Phi_2+.. \quad (40)$$

where $p<1$

More so, introducing the concept of the Binomial expansion in the simplification/expansion of the resulting nth-order chemical reaction, wherein:

$$(r+s)^n=r^n s^0+{}^nC_1 r^{n-1}s^1+{}^nC_2 r^{n-2}s^2+\ldots+{}^nC_p r^{n-p}s^p+r^0 s^n$$

such that

$$(\Phi_o+p\Phi_1+..)^n=\Phi_o{}^n(p\Phi_1)^0+{}^nC_1\Phi_o{}^{n-1}(p\Phi_1)^1+\ldots+\Phi_o{}^0(p\Phi_1)^n$$

and

$${}^nC_1=\frac{n!}{(n-1)!1!}=\frac{n(n-1)!}{(n-1)!1!}=n, n\neq 0$$

Therefore,

$$(\Phi_o+p\Phi_1+..)^n=\Phi_o{}^n+pn\Phi_o{}^{n-1}\Phi_1+\ldots \quad (41)$$

Also, for simplicity, we take:

$$\frac{1}{1+\xi\Theta}=\frac{M}{p^0+p^0\xi\Theta_o+\xi\left(p\Theta_1+p^2\Theta_2\right)}\approx\frac{M}{1+\xi\Theta_o} \quad (42)$$

Substituting equations (38) - (42) into equations (35) - (37), and (27) and (28), and expanding, where necessary, and equating the coefficients of order of p gives:

p^0:

$$f_o'''=0 \quad (43)$$

$$\frac{1}{\Pr}\left(1+\frac{4}{3}Ra\right)\Theta_o''=0 \quad (44)$$

$$\frac{1}{Sc}\Phi_o''=0 \quad (45)$$

p:

$$f_1'''=-\left(\frac{1}{2}\eta+s\right)f_o''+\left(1+\frac{F_s}{Da}\right)f_o'^{2}+\left(\frac{M}{1+\xi\Theta_o}+\frac{1}{Da}\right)f_o'-Gr\Theta_o\cos\phi-Gc\Phi_o\cos\phi \quad (46)$$

$$\frac{1}{\Pr}\left(1+\frac{4}{3}Ra\right)\Theta_1''=-\left(\frac{1}{2}\eta+s\right)\Theta_o'+f_o'\Theta_o-Ec\left(\frac{M}{1+\xi\Theta_o}\right)f_o'^{2}-Q_1\Phi_o' \quad (47)$$

$$\frac{1}{Sc}\Phi_1''=-\left(\frac{1}{2}\eta+s\right)\Phi_o'+f_o'\Phi_o+\Phi_o{}^n \quad (48)$$

p^2:

$$f_2'''=-\left(\frac{1}{2}\eta+s\right)f_1''+2\left(1+\frac{F_S}{Da}\right)f_o'\,f_1'$$
$$+\left(\frac{M}{1+\xi\Theta}+\frac{1}{Da}\right)f_1'-Gr\Theta_1\cos\phi \quad (49)$$
$$-Gc\Phi_1\cos\phi$$

$$\frac{1}{\Pr}\left(1+\frac{4}{3}Ra\right)\Theta_2''=-\left(\frac{1}{2}\eta+s\right)\Theta_1'+f_o'\Theta_1$$
$$+f_1'\Theta_o-2Ec\left(\frac{M}{1+\xi\Theta}\right)f_o'\,f_1'-Q_1\Phi_1' \quad (50)$$

$$\frac{1}{Sc}\Phi_2''=-\left(\frac{1}{2}\eta+s\right)\Phi_1'+f_o'\Phi_1+\delta n\Phi_o{}^{n-1}\Phi_1 \quad (51)$$

with the boundary conditions:

$$f_o=s,\Theta_o=1,\Phi_o=1 \text{ at } \eta=0 \quad (52)$$
$$f_o=0,\Theta_o=0,\Phi_o=0 \text{ at } \eta\to\infty \quad (53)$$
$$f_1=0,\Theta_1=0,\Phi_1=0 \text{ at } \eta=0 \quad (54)$$
$$f_1=0,\Theta_1=0,\Phi_1=0 \text{ at } \eta\to\infty \quad (55)$$
$$f_2=0,\Theta_2=0,\Phi_2=0 \text{ at } \eta=0 \quad (56)$$
$$f_2=0,\Theta_2=0,\Phi_2=0 \text{ at } \eta\to\infty \quad (57)$$

Equations (43) - (57) are solved using Mathematica 11.2 computational software. The solutions of the concentration, temperature, velocity, Sherwood number, Nusselt number, and wall shear stress are obtained.

3.2 Results and Discussion

The effects of suction, order of chemical reaction, Forchheimer number, electrical conductivity, Prandtl number, Raleigh number, rate of chemical reaction, Schmidt number, heat generation/absorption, magnetic field, and angles of inclination are investigated. For constant values of $\mu=1$, Da =1, Gr=5, Gc=5, and varied values of the chosen parameters, we obtained the results presented in Figure 2, Figure 3, Figure 4, Figure 5, Figure 6, Figure 7 Figure 7, Figure 8, Figure 9, Figure 10, Figure 11, Figure 12 and Figure 13 also in Table 1, Table 2, Table 3, Table 4 in Appendix as well as Table 5 and Table 6.

The effects of suction on the flow are seen in Figure 2, Figure 3, Figure 4. They show that the increase in the suction parameter causes fluctuation in the concentration and temperature structures, but increases the flow velocity, rate of heat transfer to the fluid, rate of mass/species transfer to the fluid, and force on the surface wall. Figure 2 depicts that the increase in the suction parameter causes fluctuation in the concentration structure. As the suction parameter increases, the concentration decreases in the region $3<\eta<4$, then turns 6 i78around and increases in the region $3<\eta<5$.

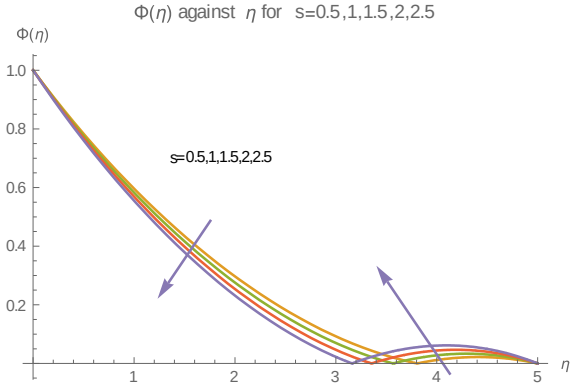

Fig. 2: Concentration-Suction Profiles

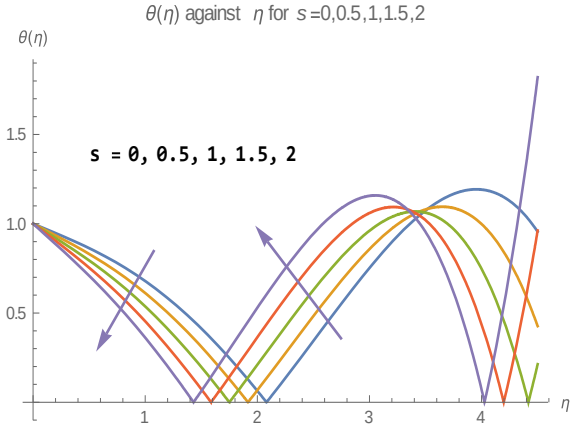

Fig. 3: Temperature-Suction Profiles

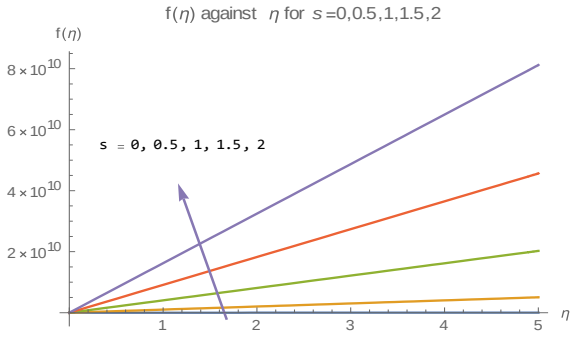

Fig. 4: Velocity-Suction Profiles

More so, Figure 3 depicts that the increase in the suction causes fluctuation in the fluid temperature structure. The temperature decreases in the region $1.2<\eta<2.2$, then turns around and increases in the region $1.2<\eta<4.6$. Furthermore,

Figure 4 depicts that the increase in the suction parameter increases the fluid velocity. Suction implies the movement of fluid from the region of lower pressure to the region of higher pressure. The pressure outside the flow system is at equilibrium and lower than that inside. The movement of the fluid from the equilibrium region must increase the fluid inside, which must influence the flow velocity. Similarly, Table 6 depicts that the increase in the suction parameter increases the rate of heat transfer to the fluid and the force at the wall.

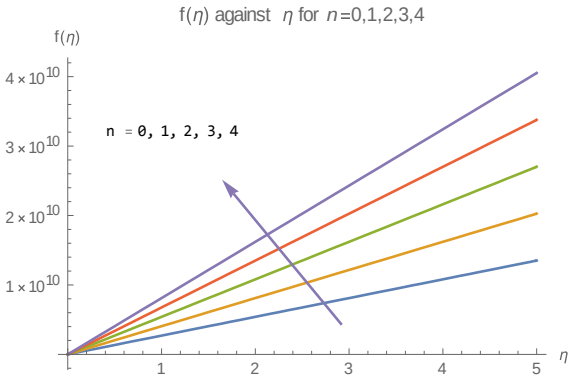

Fig. 5: Velocity- Chemical Reaction Order Parameter Profiles

The effects of chemical reaction order on the flow are shown in Table 1 (Appendix) and Figure 5. They depict that the increase in the order of chemical reaction causes fluctuation in the fluid concentration, but increases the fluid velocity. Table 1 (Appendix) depicts that the increase in the order of chemical reactions causes fluctuation in the concentration. The concentration increases in the first roll. In the second roll, it increases and drops for n=5. In the third roll, it increases and drops for n=4, 5, etc. Additionally, Figure 5 depicts that the increase in the order of chemical reactions increases the fluid velocity. The order of the chemical reaction is the sum of the powers of the active mass reactants in the rate law expression. It shows the relationship between the rate of chemical reaction and the concentration of the reacting species. Higher order depicts the strength of the relationship. Velocity is a function of concentration, which in turn is a function of the fluid particles interaction. A higher-order chemical reaction enhances the flow velocity, as seen in Figure 5.

The effects of the Forchheimer number on the flow are shown in Table 3 (Appendix) and Table 6. They show that the increase in the Forchheimer number decreases the fluid velocity, but increases the force on the wall. Table 3 (Appendix) depicts that the increase in the Forchheimer number decreases the fluid velocity. Also, Table 6 depicts that the increase in the Forchheimer number increases the force on the surface wall.

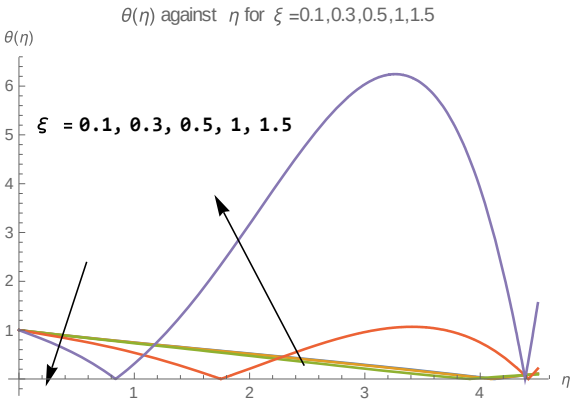

Fig. 6: Temperature- Electrical Conductivity Parameter Profiles

The effects of electrical conductivity on the flow are shown in Figure 6 and Table 6. They show that the increase in the strength of the electrical conductivity of the fluid causes fluctuation in the temperature structure, increases the rate of heat transfer to the fluid, but decreases the force on the wall. Figure 6 depicts that the increase in the Electrical conductivity parameter causes fluctuation in the temperature structure. As the Electrical conductivity parameter increases, the temperature decreases in the region $0.8 < \eta < 4.5$, then turns around and increases in the same region. The electrical conductivity of the fluid influences the fluid-particle interaction. In particular, the increase in the electrical conductivity of chemically reacting fluid leads to an increase in the fluid particle interactions, generation of electrical currents, and heat. Therefore, the fluctuation in the temperature structure may be due to some other factors. Also, Table 6 depicts that the increase in the electrical conductivity increases the rate of heat transfer to the fluid, and the force on the surface wall.

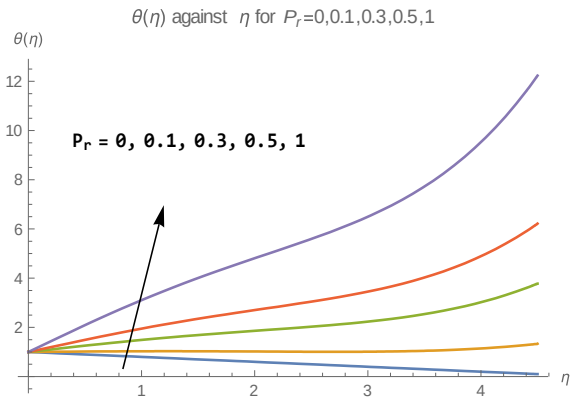

Fig. 7: Temperature-Prandtl Number Profiles

The effects of the Prandtl number on the flow are shown in Figure 7 and in Appendix in Table 4 and Table 5. They show that the increase in the Prandtl number increases the temperature and the rate of heat transfer to the fluid, causing fluctuation in the velocity, but has no effect on the force on the wall. Figure 7 depicts that the increase in the Prandtl number increases the fluid temperature. The Prandtl number is a measure of the ratio of kinematic viscosity/momentum to the thermal conductivity coefficient. Its values vary for different substances: $\Pr = 0.71$ for air, $\Pr = 1$ for electrolytic solutions, for sulphur oxide, $\Pr = 7$ for water, $\Pr = 11.6$ for water at 4 degrees Centigrade, [10]. Furthermore, the Prandtl number is used to measure the thermal diffusivity of gases at high temperatures, where it is difficult to measure experimentally due to the formation of convection currents. $\Pr < 1$ implies that the thermal diffusivity coefficient of the fluid is higher than the kinematic viscosity of the fluid, and vice versa for $\Pr \geq 1$. It has the potency of increasing the temperature. Figure 7 depicts that fluid temperature increases as the Prandtl number increases. Also, Table 4 (Appendix) depicts that the increase in the Prandtl number causes fluctuation in the velocity structure. As the Prandtl number increases the velocity increases for $0 < \Pr \leq 0.5$, then turns around, and decreases for $\Pr \geq 1$. Similarly, Table 6 depicts that the increase in the Prandtl number increases the rate of heat transfer to the fluid, but decreases the force on the wall.

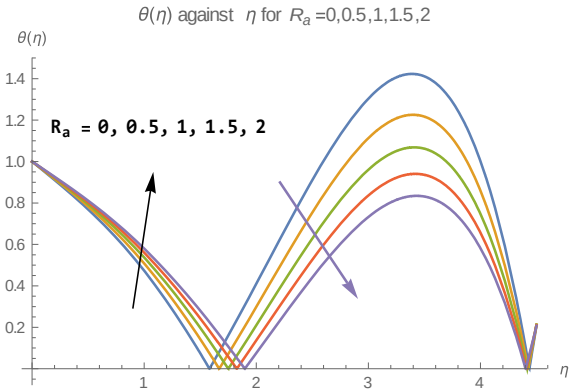

Fig. 8: Temperature- Raleigh Number Profiles

The effects of Raleigh number on the flow are shown in Figure 8 and in Appendix in Table 5 and Table 6. They show that the increase in the Raleigh number causes fluctuation in the temperature structure; increases the velocity and the rate of heat transfer to the fluid, but has no effect on the stress/force on the wall. Figure 8 depicts that the increase in the Raleigh number causes fluctuation in the temperature structure. As the Raleigh number increases, the temperature increases in the region $0 < \eta < 2$, then turns around and decreases in the region $2 < \eta < 5$. Rayleigh number is the ratio of buoyancy to inertia, and its value depends on the temperature difference between the heated plate/surface and the fluid and the characteristic length of the enclosed space. It has the potency of increasing the fluid temperature. Therefore, the fluctuation in the temperature may be due to some other factors. Also, Table 5 (Appendix) depicts that the velocity decreases with the increase in the Raleigh number. Additionally, Table 6 depicts that the increase in the Raleigh number increases the rate of heat transfer to the fluid, but has no effect on the force on the wall.

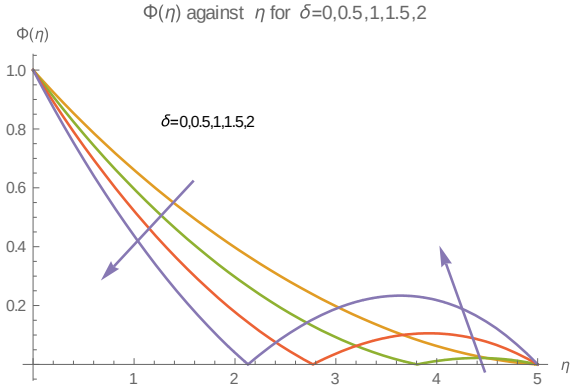

Fig. 9: Concentration-Chemical Reaction Rate Parameter Profiles

The effect of chemical reaction on the flow is shown in Figure 9. It shows that the increase in the chemical reaction rate causes fluctuation in the concentration structure. As the rate chemical reaction parameter increases the concentration decreases in the region $2 < \eta < 5$, then turns around and increases in the same region. Chemical reaction rate is the speed with which a chemical reaction takes place, and is proportional to the increase in the concentration of a product formed per unit time, or is proportional to the decrease in the concentration of the reactants per unit time. Therefore, the fluctuation in the concentration may be due to some other factors.

The effect of the chemical reaction parameter on the flow is shown in Figure 10. It shows that the increase in the Schmidt number causes fluctuation in the concentration structure. As the Schmidt number increases, the concentration decreases in the region $0 < \eta < 5$, then turns around and increases in the same region. Schmidt number is a measure of the kinematic viscosity/momentum diffusion to the molecular/mass diffusivity.

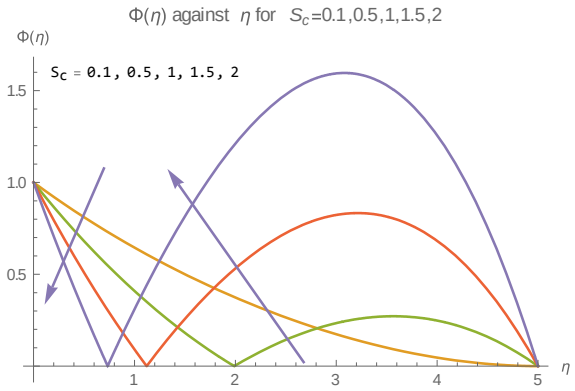

Fig. 10: Concentration-Schmidt Number Profiles

It shows how efficiently solutes are transported by diffusion, and has the potency of enhancing the fluid concentration. Its values vary for different substances: $Sc = 0.22$ for hydrogen, $Sc = 0.66$ for water vapour, $Sc = 0.78$ for ammonia, and $Sc = 0.95$ for carbon dioxide, [10]. High values imply that the momentum diffusion of the fluid is higher than the mass diffusivity, and vice versa. A Schmidt number unity or close to unity means that the kinematic viscosity and mass diffusion of the fluid are equal, or that kinematic viscosity and mass diffusivity occur at the same rate, such that both are equally effective. Therefore, with the ability to enhance the fluid concentration, the fluctuating structure here may be caused by some other factors.

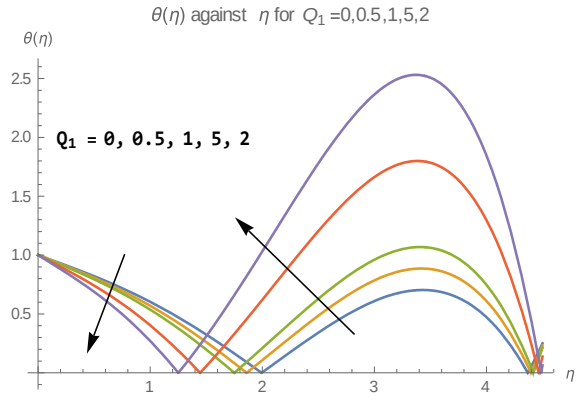

Fig. 11: Temperature-Heat Generation/Absorption Parameter Profiles

The effect of heat generation/absorption on the fluid temperature is shown in Figure 11. It depicts that the increase in the heat generation/absorption parameter (Q_1) causes fluctuation in the temperature structure. As the heat generation/absorption parameter increases, the temperature decreases in the region $1.2 < \eta < 2$, then turns around and increases in the region. $Q_1 > 0$ indicates heat generation, while $Q_1 < 0$ indicates heat absorption. The increase in the heat generation parameter has the potency of increasing the fluid temperature, and force on the surface wall, but decreases the rate of heat transfer to the fluid. The converse is the case for heat absorption. Therefore, the fluctuation in the fluid temperature structure may be due to some other factors.

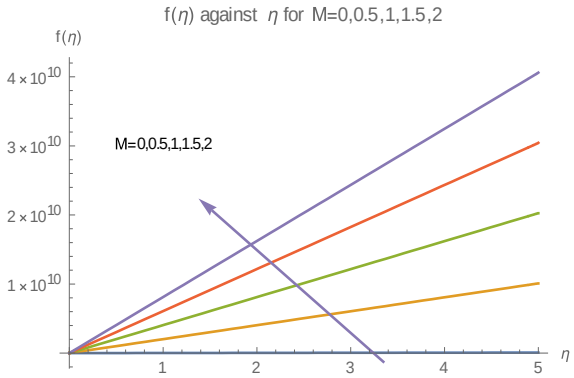

Fig. 12: Velocity-Magnetic Field Parameter Profiles

The effect of the Magnetic Field parameter on the flow is shown in Figure 12. It shows that the increase in the Magnetic Field parameter increases the fluid velocity. Being chemically reactive, the fluid is electrolytic, and as such its particles exist as ions/charges; therefore, it is magnetically susceptible. The motion of these ions in the magnetic field produces electric currents, and the action of the magnetic field on the electric current produces the mechanical force (called the Lorentz force), which has the potency of freezing the fluid velocity. Therefore, the increase in the fluid velocity may be due to some other factors.

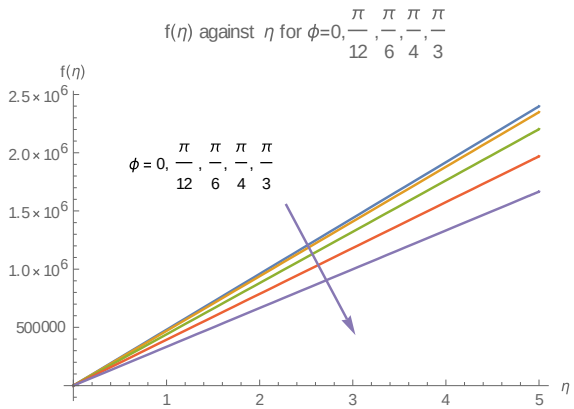

Fig. 13: Velocity-Inclined Angle Profiles

The effect of the inclined angle on the flow is shown in Figure 13. It shows that the increase in the inclined angle decreases the fluid velocity. This is consonance with [1], [2], [3], [4], [5], [6], [7], [8], [9], [10], [11], [12], [13], [14], [15], [16], [17], [18], [19].

Table 6. Sherwood Number, Nusselt Number, and Skin Friction- Suction, Forchheimer number, Electrical conductivity, Prandtl number, and Raligh number Relations

Parameters	$-\Phi'(0)$	$-\Theta(0)$	$C_f(0)$
s			
0.0	0.44939	0.26515	17261.77
0.5	0.46521	0.32907	17261.95
1.0	0.48135	0.40143	17261.14
1.5	0.49781	0.48226	17261.34
2.0	0.51459	0.57161	17261.55
F_h			
0			17261.08
0.5			17261.11
1.0			17261.14
3.0			17261.27
5.0			17261.39
ξ			
0.1		0.27911	12515.60
0.3		0.28139	17024.51
0.5		0.28883	17203.70
1.0		0.40143	17261.14
1.5		0.88317	17270.22
P_r			
0.0		0.20000	17261.14
0.1		0.38004	17261.14
0.3		0.51491	17261.14
0.5		0.99302	17261.14
1.0		2.19354	17261.14
Ra			
0.0		0.44942	17261.14
0.5		0.42287	17261.14
1.0		0.40143	17261.14
1.5		0.39374	17261.14
2.0		0.36891	17261.14

4 Conclusion

Unsteady high-speed MHD natural convective flow over an inclined plate with variable electrical conductivity, higher-order chemical reaction, thermal radiation, and concentration gradient-dependent heat generation/absorption is examined. The analysis of results shows that the increase in the

- Suction parameter causes fluctuation in the fluid concentration, temperature, and wall shear stress, but increases the flow velocity, rate of heat transfer, and the rate of mass transfer.
- Order of chemical reaction parameters causes fluctuation in the fluid concentration structure, but increases the flow velocity.
- Forchheimer number decreases the fluid velocity but increases the force on the wall.
- Electrical conductivity causes fluctuation in the temperature structure, increases the rate of heat transfer to the fluid, but decreases the force on the wall
- Prandtl number increases the temperature and the rate of heat transfer to the fluid, causes fluctuation in the velocity but has no effect on the force on the wall
- Raleigh number causes fluctuation in the temperature structure; decreases the fluid velocity and the rate of heat transfer to the fluid, but has no effect on the force on the wall
- Chemical reaction rate causes fluctuation in the concentration structure
- Schmidt number causes fluctuation in the concentration structure
- Heat generation/absorption parameter causes fluctuation in the temperature structure
- Magnetic field parameter increases the fluid velocity
- Inclined angle decreases the fluid velocity.

References:

[1] Makinde O.D., MHD mixed-convection interaction with thermal radiation 500tion and nth order chemical reaction past a vertical porous plate embedded in a porous medium, *Chemical Engineering Communication,* Vol. 198, No, 4, 2011, pp. 590-608. doi: 10.1080/00986445.2010.500151.

[2] Imoro R., Arthur E.M. and Seini Y.I., Heat and mass transfer over a vertical surface with convective boundary condition in the presence of viscous dissipation and nth-order chemical reaction, *International Journal of Computation and Applied Mathematics,* Vol. 9, No, 2, 2014, pp. 101-118.

[3] Kharabela S., Sampada K.P., and Gouranga C.D., Higher-order chemical reaction effects on MHD Nanofluid flow with slip boundary conditions: a numerical approach, *Mathematical Modelling of Engineering Problems,* Vol. 6, No, 2, 2019, pp. 293-299. doi: doi.org/10.18280/mmep.0602

[4] Shrama P.R. and Singh G., Steady MHD natural convective flow with variable electrical conductivity and heat generation along an isothermal vertical plate, *Tankang Journal of Science and Engineering,* 13, Vol. 13, 2010, pp. 235-242. doi: 10.1007/s13370-015-0372-1.

[5] Alam M.S. and Ahammad M.U., Effects of variable chemical reaction and variable electric conductivity on free convective heat and mass transfer flow along an inclined stretching sheet with variable heat and mass fluxes under the influence of Dufour and Soret effects, *Nonlinear Analysis: Modeling and Control,* 16, Vol. 16, 2011, pp.1-16. doi: 10.15388/NA.16.1.14110

[6] Chakraborty S. and Medhi N., Effects of permeability and heat generation on MHD flow along a vertical isothermal porous plate under variable electrical conductivity, *International Journal of Advanced Research,* 2016, pp. 764-775. doi: 10.21474/IJAR01/1855.

[7] Desale S.V. and Pradhan V.H., Implicit finite difference solution of MHD boundary layer heat transfer over a moving plate, *IOSR Journal of Mathematics,* 9, Vol. 9, 2013, pp.18-23.

[8] Mishra S.R. and Jena S., Numerical solution of boundary layer MHD flow with viscous dissipation, *The Scientific World Journal,* 2014, pp. 1-5. doi: doi.org/10.1155/2014/756498.

[9] Haque M.M. and Sarder U.K., Thermal diffusion effect on convective heat and mass transfer of high-speed MHD flow over a stretching sheet, *Journal of Scientific Research and Reports,* Vol. 8, 2015, pp.1-14. doi: doi.org/10.9734/JSRR/2015/18075.

[10] Arifuzzaman S.M., Khan M.S., Mehedi M.F.U., Rana B.M.J. and Ahmed S.F. (2018), Chemically reactive and natural convective high-speed MHD fluid flow through an oscillatory vertical porous plate with heat and radiation absorption, *Journal of Engineering Science and Technology,* Vol. 21, 2018, pp. 215-228.

[11] Bhuvaneswari M.S.S. and Kim Y.J., Exact analysis of radiation convective flow with heat and mass transfer over an inclined plate in a porous medium, *World Applied Journal,* 10, Vol. 10, 2010, pp. 774-778. doi: doi:10.2478/ijame-2020-0036.

[12] Redd M.G. and Reddy, M.C.K., Mass transfer and heat generation effects on MHD free convective flow past an inclined vertical surface in a porous medium, *Journal of Applied Fluid Mechanics,* Vol. 4, No. 1, 2011, pp. 7-11.

[13] Gnaneswara R.M., Lie analysis of heat and mass transfer effects on a steady MHD free convective dissipative fluid flow past an inclined porous surface with heat generation, *Journal of Applied Fluid Mechanics,* Vol. 39, No. 3, 2012, pp. 233-254. doi: 10.2478/ijame-2020-0036.

[14] Narayana S.P.V. and Sravanthi, S., Influence of variable permeability on unsteady MHD convection flow past a semi-infinite inclined plate with thermal radiation and chemical reaction, *Journal of Energy Heat Mass Transfer,* Vol. 34, 2012, pp. 143–161. doi: 10.1016j.jppr.2015.07.002.

[15] doi:Saidual Islam M.D., Samuzzoha M.D., Ara S., and Dey P., MHD free convective flow and mass transfer flow with heat generation through an inclined plate. *Annals of Pure and Applied Mathematics,* Vol. 3, 2013, pp. 129-141. doi: doi.org/10.2478/ijame-2022-0040.

[16] Islam Manjiul, Farjana Akter, Ariful Islam,with porous medium, *American Journal of Applied Mathematics,* Vol. 3, No. 5, 2015, pp. 215-220. doi: doi.org/10.1016/j.jestch.2018.03.004.

[17] Baiyeri J.F., Esan O.A., Ogunbayo T.O., Enababor O.E. and Salawu S.O. (2017), Analysis of unsteady natural convective flow through an inclined plate, *Asian Journal of Physical and Chemical Science,* 2(4), Vol. 2, No. 4, 2017, pp.1-12.

[18] Pattnaik J.R., Dash G.C. and Singh S. (2017), Radiation and mass transfer effects on MHD flow through porous medium past an exponentially accelerated inclined plate with variable temperature, *Ain Shams Engineering Journal,* Vol. 8, 2017, pp. 67-75. https://doi.org/10.1016/j.asej.2015.08.014.

[19] [19] Rana B.M.J, Raju Roy, Lasker Ershad Ali, Ahammed S.F. (2017), Radiation absorption and variable electrical conductivity effects on high-speed MHD free convective flow past an exponentially accelerated inclined plate, *World Journal of Mechanics,* Vol. 7, 2017, pp. 211-241. https://doi.org/10.4236/wjm.2017.78019

[20] Sparrow E.M., Eichhorn R., and Grigg J.L., Combined forced and free convection in a boundary layer, *Physics of Fluids,* Vol. 2, 1959, pp. 319-320. doi: 10.1063/1.1705928.

[21] Das U.N., Deka R.K., Soundalgekar V.M., Effects of mass transfer on flow past an impulsively started infinite vertical plate with constant heat flux and chemical reaction, Forsch. Ingenieurwes, Vol. 60, 1994, pp. 284–287.

[22] Muthucumaraswamy R. and Ganesan P. (2001), First-order chemical reaction on flow past an impulsively started vertical plate with uniform heat and mass flux, *Acta Mechanica,* Vol. 147, 2001, pp. 45-57.

[23] Muthucumaraswamy R. and Vijayalakshmi A., Radiation effects on the flow past impulsively started vertical plate with variable temperature and mass flux, *Theoretical and Applied Mechanics,* Vol. 32, No. 3, 2005, pp. 223-234

[24] Singh N.P., Kumar A., Singh A.K. and Singh Aul K., MHD free convective flow of viscous fluid past a porous vertical plate through a non-homogeneous porous medium with radiation and temperature gradient-dependent heat source in the slip-flow regime. *Ultra Science,* 18, Vol. 18, No. 3, 2006.

[25] Makinde D.O. and Ogulu A., The effects of thermal radiation on the heat and mass transfer flow of a variable viscosity fluid flow past a vertical porous plate permeated by a transverse magnetic field, *Chemical Engineering Communication,* Vol. 195, No. 12, 2010, pp. 1575-1584. doi: 10.1080/00986440802115549.

[26] Rajput U.S. and Kumar S., MHD flow past an impulsively started vertical plate with variable temperature and mass diffusion, *Journal of Applied Mathematical Sciences,* Vol. 5, No. 3, 2011, pp.149-157.

[27] Gharan N, Das S, Maji S.L., and Jana R.N., Effects of radiation on MHD free convection flow past an impulsively moving vertical plate with ramped wall temperature, *American Journal of Scientific and Industrial Research,* Vol. 3, No. 6, 2012, pp. 376–386 doi: 10.5252/ajsir/2012.3.6.376.386

[28] Rajput U.S. and Kumar S., Radiation effects on MHD flow past an impulsively started vertical plate with variable heat and mass transfer, *International Journal of Applied Mathematics and Mechanics,* Vol. 8, 2012, pp. 66-85.

[29] Sharma S. and Deka R.K., Chemical reaction effects on MHD mixed convection flow of water at maximum density past a vertical plate under variable temperature, *IORS Journal of Applied Physics,* Vol. 1, 2012, pp. 1-7.

[30] Sharma B.K., Yadav K., Mishra N.K. and Chaudhary R.C., Soret and Dufour effects on unsteady MHD mixed convection flow past a radiative vertical porous plate embedded in a porous medium with chemical reaction, *Applied Mathematics,* Vol. 3, 2012, pp. 717-723. https://doi.org/10.4236/am.2012.37105.

[31] Ahmed N. and Dutta M., Transient mass transfer flow past an impulsively started vertical plate with ramped plate velocity and ramped temperature, *International Journal of Physical Sciences,* Vol. 8, No. 7, 2013, pp. 254 – 263. doi: 10.5897/IJPS12.713.

[32] Umamaheswar M., Raju M.C., Varma S.V.K and Gireeshkumar J. (2016), Numerical investigation of MHD free convection flow of a non-Newtonian fluid past an impulsively started vertical plate in the presence of thermal diffusion and radiation absorption, *Alexandria Engineering Journal,* Vol. 55, 2016, pp. 2005-2014. https://doi.org/10.1016/j.aej.2006.07.014.

[33] Okuyade W.I.A., Abbey T.M. and Gima-Laabel A.T. (2018), Unsteady MHD free convective chemically reacting fluid flow over a vertical plate with thermal radiation, Dufour, Soret and constant suction effects. *Alexandria Journal of Engineering,* Vol. 57, 2018, pp. 3863-3871. doi: 10.1016/j.aej.2018.02.006.

[34] Okuyade W.I.A. and Okor T., Transient MHD free convective chemically reacting flow over a moving hot vertical porous plate with heat generation/absorption, thermal radiation, viscous dissipation, oscillating suction, and free stream velocity effects, *Journal of Mathematics and Computational Sciences,* Vol. 9, No. 6, 2019, pp. 739-754. doi: 1.2891/jmcs/4079.

[35] Okuyade W.I.A. and Okor T., Unsteady MHD free convective chemically reacting flow over a vertical plate with a heat source, thermal radiation and oscillating wall temperature, concentration and suction effects, *American Journal of Fluid Dynamics,* Vol. 9, No. 2, 2019, pp. 33-47. doi: 10.5923/j.ajfd.20190902.01.

[36] Ighoroje W.A. Okuyade and Mebine Promise, MHD double-diffusive and viscous dissipative boundary layer flow over a vertical plate with heat source, reacting species, and thermal and mass transfer gradients, *International Journal of Fluid Mechanics & Thermal Sciences,* Vol. 8, No. 3, 2023, pp. 64-74. doi: 10.11648/j.ijfmts.20230901.11.

[37] Ighoroje W.A. Okuyade and Tamunoimi M. Abbey, Transient MHD fluid flow past a moving vertical surface in a velocity slip flow regime, *WSEAS Transactions on Fluid*

Mechanics, Vol. 19, 2024, pp. 99-112. https://doi.org/10.37394/232013.2024.19.10.

[38] Forchheimer P., Wasserbewgung durch Bden, 45th Edition, *Zeitschrift des Vereins deutcher Ingenieure, Dusseldorf*, 1901.

[39] Yao Y.D., Li G.Z., Qin P.F., Seepage features of high-velocity non-Darcy flow in highly productive reservoirs, *Journal Natural Gas Science and Engineering,* Vol. 27, No. 3, 2015, pp. 1732-1738e. doi: 10.1016/j.jngse.2015.10.039.

[40] Chen Y.F., Zhou J.Q., Hu S.H., Hu R., Zhou C.B., Evaluation of Forchheimer equation coefficients for non-Darcy flow in deformable rough-walled fractures, *Journal of Hydrology,* Vol. 529, No. 3, 2015, pp. 993-1006.

[41] Dukhan N, Patel K., Effect of sample length on flow properties of open-cell metal foam and pressure-drop correlations. *Journal of Porous Materials,* Vol. 18, No. 6, 2011, pp. 655-665. doi: 10.1007/s10934-010-9423-z

[42] Okuyade W.I.A., Abbey T.M. and Abbey M.E., Application of Dupuit-Forchheimer model to groundwater flow into a well, *Modelling Earth Systems and Environment (Springer),* 2021. https://doi.org/10.1007//s-40808-021-01224-2.

[43] Yian L.Y. Ahmad S. and Pop I., Unsteady separated stagnation-point flow with suction towards a stretching sheet, *AIP Proceedings,* Vol. 1602, 2014, pp. 317. doi: 10.1063/1.4882505.

[44] Momani S., Erjaee G.H., The modified homotopy perturbation method for solving strongly non-linear oscillators, *Computers and Mathematics with Applications,* Vol. 58, 2009, pp. 2209-2220. doi: 10.1016/j.camwa.2009.03.082.

Contribution of Individual Authors to the Creation of a Scientific Article (Ghostwriting Policy)

This work is solely carried out by the author.

Sources of Funding for Research Presented in a Scientific Article or Scientific Article Itself

This research did not receive any specific grant from funding agencies in the public, commercial, or not-for-profit sectors.

Conflict of Interest

The authors have no conflicts of interest to declare.

APPENDIX

Table 1. Concentration-Chemical Reaction Order Relation

Φ	$\Phi(n=1)$	$\Phi(n=2)$	$\Phi(n=3)$	$\Phi(n=4)$	$\Phi(n=5)$
1	0.59620	0.61977	0.63212	0.63736	0.63780
2	0.29707	0.33686	0.35579	0.35836	0.34948
3	0.09238	0.14015	0.14707	0.11507	0.04667
4	0.01163	0.02918	0.03042	0.20524	0.50929
5	$3.55271*10^{-17}$	$7.10543*10^{-17}$	0.26428	0.85708	1.84169

Table 2. Velocity-Forchheimer Number Relation

f	$f(F_h=0)$	$f(F_h=0.5)$	$f(F_h=1.0)$	$f(F_h=3.0)$	$f(F_h=5.0)$
0.0	$4.05199*10^{9}$	$4.05190*10^{9}$	$4.05180*10^{9}$	$4.05143*10^{9}$	$4.05105*10^{9}$
0.5	$8.10399*19^{9}$	$8.10380*10^{9}$	$8.10361*10^{9}$	$8.10287*10^{9}$	$8.10212*10^{9}$
1.0	$1.21560*10^{10}$	$1.21557*10^{10}$	$1.21554*10^{10}$	$1.2153*10^{10}$	$1.21532*10^{10}$
3.0	$1.62080*10^{10}$	$1.62076*10^{10}$	$1.62072*10^{10}$	$1.62057*10^{10}$	$1.62042*10^{10}$
5.0	$2.02599*10^{10}$	$2.02595*10^{10}$	$2.02590*10^{10}$	$202571*10^{10}$	$2.02553*10^{10}$

Table 3. Velocity-Prandtl Number Relation

f	$f(P_r=0)$	$f(P_r=0.1)$	$f(P_r=0.3)$	$f(P_r=0.5)$	$f(P_r=1.0)$
0.0	$1.57304*10^{7}$	$5.57162*10^{8}$	$1.70295*10^{9}$	$6.83001*10^{16}$	$5.71319*10^{9}$
0.5	$3.14557*10^{7}$	$1.11433*10^{9}$	$3.40590*10^{9}$	$1.36609*10^{17}$	$1.142642*10^{10}$
1.0	$4.71856*10^{7}$	$1,67149*10^{9}$	$5.10884*10^{9}$	$2.04993*10^{17}$	$1.71396*10^{10}$
3.0	$6.29271*10^{7}$	$2.22864*10^{9}$	$6.81178*10^{9}$	$2.73201*10^{17}$	$2.28528*10^{10}$
5.0	$7.86843*10^{7}$	$2.78578*10^{9}$	$8.51470*10^{9}$	$3.41501*10^{17}$	$2.85659*10^{10}$

Table 4. Velocity-Raleigh Number Relation

f	$f(Ra=0)$	$f(Ra=0.5)$	$f(Ra=1.0)$	$f(Ra=1.5)$	$f(Ra=2.0)$
0.0	$4.06735*10^{9}$	$4.05958*10^{9}$	$4.05180*10^{9}$	$4.04404*10^{9}$	$4.03625*10^{9}$
0.5	$8.13471*10^{9}$	$8.11916*10^{9}$	$8.10361*10^{9}$	$8.08861*10^{9}$	$8.07251*10^{9}$
1.0	$1.22021*10^{10}$	$1.21787*10^{10}$	$1.21554*10^{10}$	$1.21321*10^{10}$	$1.21088*10^{10}$
1.5	$1.62694*10^{10}$	$1.62383*10^{10}$	$1.62072*10^{10}$	$1.61761*10^{10}$	$1.61450*10^{10}$
2.0	$2.03367*10^{10}$	$1.02979*10^{10}$	$2.02590*10^{10}$	$2.02201*10^{10}$	$2.01812*10^{10}$